Indian Journal of Biochemistry & Biophysics
Vol. 63, September 2026, pp. 1020-1035
DOI: 10.56042/ijbb.v63i9.22779

Neuroprotective role of hydroxychloroquine and trimebutine in alzheimer's disease: Network pharmacology and molecular simulations

Renukaradhya Maharudraiah[1], Krishna Kant[2], Madhusudhan Reddy Alimeneti[3], Roma Kumari Gupta[4], Sunil Kumar Kurmi[4], Santosh Prasad Chaudhary Kurmi[4], Aleesha Mujeeb Shaheen[5] & Mahalakshmi Suresha Biradar[5]*

[1]Department of Pharmacology, KLE College of Pharmacy, Bengaluru-560010, KLE Academy of Higher Education and Research, Belagavi-590 010, Karnataka, India

[2]Department of Biosciences and Biotechnology, Indian Institute of Technology Kharagpur-721 302, West Bengal, India

[3]Department of Pharmacognosy, Princeton College of Pharmacy, Ghatkesar, Hyderabad-501 301, Telangana, India

[4]Department of Pharmacy, Universal College of Medical Sciences, Bhairahawa-32900, Nepal

[5]Department of Pharmaceutical Chemistry, Al-Ameen College of Pharmacy, Bengaluru-560 027, Karnataka, India

Received 15 August 2025; *revised 06 May 2026*

Alzheimer's disease (AD) is the most common neurodegenerative pathology worldwide and is marked by the progressive loss of neurons. The current therapeutic armamentarium, which is composed mostly of cholinesterase inhibitors, only provides symptomatic amelioration and is often plagued with undesirable adverse events when chronically administered. Consequently, identification of safer and more efficacious therapeutic alternatives is imperative. Drug repurposing is an inexpensive and time-saving way to uncover new clinical uses for already existing pharmacological agents in the context of AD management. In the current study, an integrated *in silico* approach consisting of network pharmacology, molecular docking, molecular dynamics (MD) simulation, gene expression profiling using AlzData and cell permeability analysis was used to evaluate the therapeutic efficacy of Trimebutine and Hydroxychloroquine against Alzheimer's disease. The probable target proteins' protein-protein interaction (PPI) network demonstrated non-random connectedness, indicating strong functional linkages. The KEGG pathway enrichment analysis showed that PI3K and Akt are involved in endothelial growth factor (VEGF)-mediated angiogenesis, longevity regulation, and gefitinib resistance pathways, suggesting possible roles in neuroprotection and vascular health. Molecular docking experiments indicated that Trimebutine had a strong sequence homology with 5UBR and 2Y3A, with binding energies of -7.3 and -7.2 kcal/mol, respectively, whereas Hydroxychloroquine bound to 2Y3A at a greater level (-7.0 kcal/mol). Molecular dynamics (MD) simulation validated the stability of the docked complexes, characterized by low RMSD trajectories and persistent hydrogen bond interactions. Both drugs had passive membrane permeability limits, while hydroxychloroquine was somewhat more membrane affine. Trimebutine and Hydroxychloroquine established stable interactions against AD key targets, especially in the PI3K-Akt system, thereby supporting their candidature as repurposed therapeutics for Alzheimer's disease.

Keywords: Alzheimer's disease, Docking, Hydroxychloroquine, MD Simulation, Trimebutine

Alzheimer's disease (AD) is a progressive neurodegenerative disease that is characterised by issues in memory, cognitive functioning and failure to perform normal functions. It includes the most prevalent type of dementia that primarily affects the elderly and is referred to as the fourth leading cause of death in the world[1]. From the burden of dementia, in 2021, the World Health Organization reports that around 57 million people were suffering from dementia, with most of them living in low and middle-income countries[2]. These are caused by 60-70% by Alzheimer's disease. Dementia remains a major cause of mortality and disability, and it is estimated that in 2019, the global cost of dementia was US $ 1.3 trillion[3]. Women endure uneven morbidity, delivering 70% of the care, and exhibit higher rates of morbidity and disability[4]. Amyloid-beta (Aβ) plaque deposition, neurofibrillary tangles (NFTs), neuronal loss, neuroinflammation and marked synaptic alterations are the pathophysiological hallmarks of AD[5]. The disease is commonly reported to cause symptoms of disorientation, confusion, mood instability and lack of speech, swallowing and ambulation, as the disease progresses through empirical observation[6]. There is currently no definite cure or

*Correspondence:
Phone: +91-9620803093 (Mob)
E-mail: mahalakshmisb12@gmail.com
Suppl. data available on respective page of NOPR

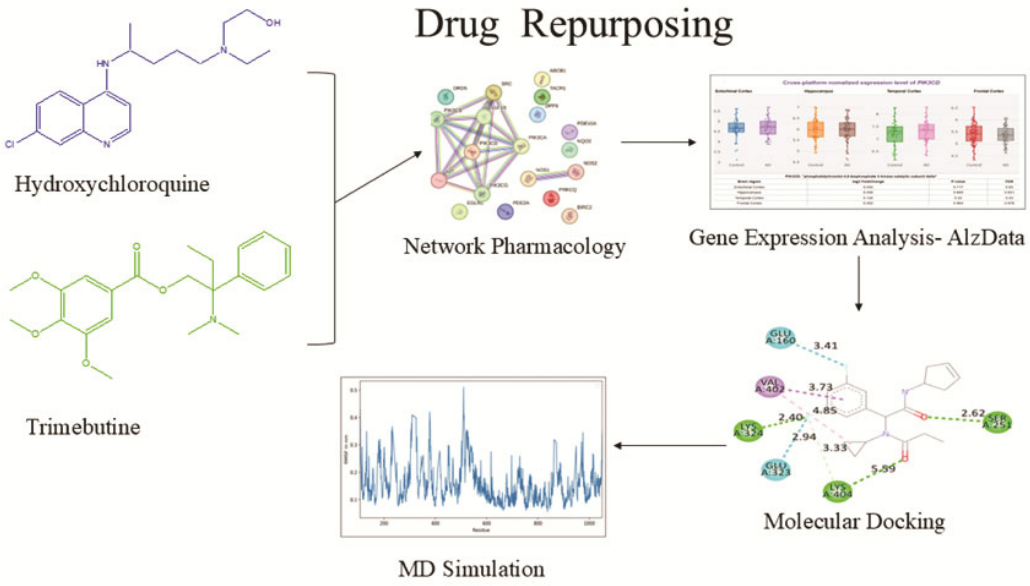

Graphical abstract

disease-modifying treatment available, and, as a result, the treatment options are based on pharmacological therapy, primarily acetylcholine esterase inhibitors (donepezil, galantamine, rivastigmine) and N-methyl-D-aspartate (NMDA) receptor inhibitors (memantine), most of which are used to treat the symptoms in palliative treatment[7]. Regardless of these efforts, there are symptomatic improvements without altering the disease process, and the necessity to develop new therapeutic options becomes urgent.

FDA-approved medications hydroxychloroquine (HCQ) and trimebutine are used to treat conditions including malaria, autoimmune illnesses (such as rheumatoid arthritis and systemic lupus erythematosus), and gastrointestinal motility issues[8,9]. Their proven safety history and diversity of pharmacodynamic properties have provoked the desire to repurpose these drugs to the neurodegenerative setting, including AD[10]. Emerging pre-clinical evidence suggests that these anti-inflammatory, neuroprotective and cell signalling modulatory effects of these compounds might be beyond traditional indications[11,12].

Varma *et al*. (2023) showed that HCQ rescues dysfunctional hippocampal synaptic plasticity and modulates late long-term potentiation (LTP) in an appetitive dose-dependent fashion in APP/PS1 transgenic mice before the emergence of explicit accumulation of amyloid and neurodegeneration. HCQ lowers neuroinflammation, increases microglial clearance of the β-amyloid, and presumably also lowers tau phosphorylation *in vitro* phenotypic assays. Mechanistically, the activation of the transcription factor, STAT3, was identified to be inhibited by HCQ in astrocytes, neurons and microglia, which is the probable mechanism of its neuroprotective action in AD pathogenesis[13].

Akkaya *et al*. (2023) identified that trimebutine showed the best *in vitro* acetylcholinesterase (AChE) inhibitory effect in the screening of FDA-approved drugs, 68.70 ± 0.46% at 1000 µM of concentration. A good AChE binding inhibitor was indicated by molecular docking, whereas a CNS activity predictive AD study using trimebutine indicated its applicability in AD. Its anti-inflammatory action was further detailed by Ogawa *et al*., who inhibited Toll-like receptor (TLR) 2, 4, 7, 8 and 9 signalling, decreased IL-6. IL-6 and other pro-inflammatory cytokines enhanced survival by using a murine sepsis model[12]. In addition to acting on neuroinflammation, trimebutine can have an impact on the gut-brain axis, which can be used to mitigate the neurodegeneration caused by *H. pylori* by restoring gastrointestinal motility, suppressing inflammation and correcting dysbiosis[14].

The overall aim of the current investigation is to use an integrated computational approach, which is a combination of network pharmacology, molecular docking and molecular dynamics, to define multi-target mechanisms of HCQ and trimebutine in Alzheimer's disease. Through the identification of the important protein targets, signalling pathways and ligand-inspired

interactions, we will seek to offer a mechanistic explanation to support the repurposing of these agents as potential therapeutic candidates for AD.

Materials and Methods

Selection of compound

The choice of candidate drugs was based on their known pharmacological characteristics and new evidence of their possible therapeutic applicability in Alzheimer's disease. Hydroxychloroquine and trimebutine have been studied in the past, both *in vitro* and *in vivo* models, and their potential and possible applications in neuroprotection are highlighted. These compounds were chosen to study their mechanisms of action at a molecular level by *in silico* analysis[12,13]. The three-dimensional (3D) structures of hydroxychloroquine and trimebutine were obtained from the PubChem database (https://pubchem.ncbi.nlm.nih.gov/) to carry out a further *in silico* analysis (Fig. 1).

Screening of targets associated with compounds

Disease-associated targets for both hydroxychloroquine and trimebutine were predicted using the web tool of Swiss Target Prediction (https://www.swisstargetprediction.ch/). The 3D structures of the compounds were uploaded, and the organism was configured as homo sapiens to ensure exclusive retrieval of targets that are exclusive to humans. To increase prediction reliability, only targets with a probability score of 0.1 or higher were considered, and low-confidence predictions were not used. The redundant targets were eliminated, and the target set was further analyzed[15].

Profiling of genes related to alzheimer's disease

The keyword "Alzheimer's" was used to search the GeneCards database (https://www.genecards.org/), identifying the genes related to the progression of this disease. GeneCards is a diagnostic tool that combines an extensive searchable database of genomic, transcriptomic, proteomic, genetic, clinical and functional information from around 200 sources. Gene filtering was performed to obtain biologically relevant genes with relevance score ≥ 10. Uncategorized genes, pseudogenes and low-confidence genes were removed. The filtered set of genes was taken into consideration for further intersection and network analysis[16].

Establishing networks of protein-protein interactions (PPIs)

The overlapping targets between drug-related and disease-related datasets were identified using Venn analysis. These shared targets were considered potential therapeutic targets for further network construction and analysis. The intersecting proteins were then retrieved and analysed to build a PPI network using the STRING database (https://string-db.org/)[17]. The analysis was based on Homo sapiens as the organism and a high confidence interaction score threshold of 0.70. The resulting PPI network was visualised and further analysed with the help of Cytoscape software (version 3.10.2). The CytoHubba plugin in Cytoscape was used to determine hub genes to identify the top 10 most connected genes in the network[18].

Kyoto encyclopaedia of genes and genomes (KEGG) Pathway study of enrichment and gene ontology (GO)

The top 10 genes obtained using Cytoscape v3.10.2 were subjected to GO and KEGG enrichment analyses using the ShinyGo 0.82 server (https://bioinformatics.sdstate.edu/go82/). Both analyses used a false discovery rate (FDR) cutoff p-value of <0.05. GO analysis classified enriched terms into three major categories - Biological Process (BP), Molecular Function (MF) and Cellular Component (CC). KEGG pathway enrichment provided important information on signalling pathways, giving a general overview of the possible functions that these genes can perform in different cellular processes[19].

Verification of the AD signalling pathway's target changes: The AlzData database

Gene expression profiles obtained from brain tissues of patients with Alzheimer's disease

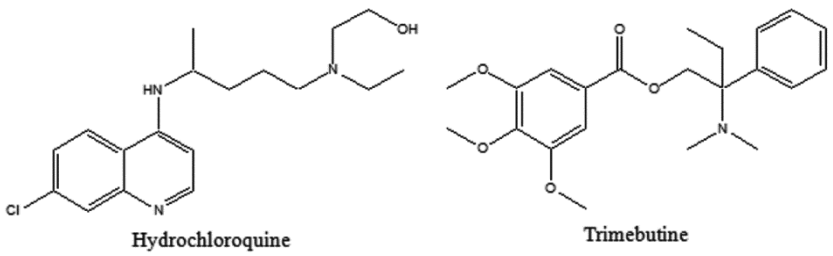

Fig. 1 — 2D structure of Hydrochloroquine and Trimebutine

were downloaded from the AlzData database (https://www.alzdata.org/). To determine changes in the activity of key signalling pathways, gene symbols were entered into AlzData for target proteins of AD, which allowed us to examine the correlations of these with known markers of AD pathology, such as tau and amyloid. Differential expression analyses were conducted to compare the AD and control samples to highlight dysregulated targets. Particular emphasis was placed on the PI3K signalling pathway, whereby patterns of gene expression of critical genes were scrutinised to identify potential contributors to AD pathogenesis and reveal targets for therapeutic intervention[20].

Protein validation

PROCHECK (https://www.ebi.ac.uk/thornton-srv/software/PROCHECK/) was used to evaluate the structural integrity analysis of the target proteins. It produced Ramachandran plots in evaluating stereochemical properties, like bond angles, torsion angles and atomic contacts, ensuring the correctness and reliability of the protein model before the molecular docking process.

Molecular docking

Based on the network pharmacology analysis, the 4 best ranking targets were chosen for docking. The top targets according to network pharmacology were PIK3CD (α), PIK3CB (β), PIK3CA (Δ), and SRC. X-ray crystallographic structures of these target proteins (PDB IDs: 5UBR, 2Y3A, 7LM2, and 8JN9, respectively) were retrieved from the Protein Data Bank (https://www.rcsb.org/). The X-ray resolution of protein structures was 5UBR-2.40Å, 2Y3A- 3.30Å, 7LM2- 2.79Å, and 8JN9- 2.72Å. Protein structures were prepared for docking by removal of co-crystallised ligands, heteroatoms and water molecules using BIOVIA Discovery Studio Visualiser. The prepared ligands were subsequently converted to PDBQT structures by using the PDB to PDBQT converter module of PyRx (version 0.8) for docking studies. Grid box dimensions along the X, Y, and Z axis were specified as stated in (Table 1) to cover the active sites[21].

Reference inhibitors were selected based on FDA-approved drugs targeting the respective proteins, including Alpelisib (PIK3CA), Idelalisib (PIK3CD), Copanlisib (pan-PI3K inhibitor), and Dasatinib (SRC kinase), to enable comparative docking analysis. Ligands were prepared by using the 3D structures of hydroxychloroquine and trimebutine downloaded from PubChem (https://pubchem.ncbi.nlm.nih.gov/) in an SDF file. Energy minimisation was done by using the MMFF94 force field present in the Open Babel module of PyRx. Structures were refined to PDBQT format. Molecular docking simulations were conducted in PyRx for the evaluation of binding poses and affinities. Post-docking analyses were performed in BIOVIA Discovery Studio 2021 to visualise and characterise important interactions such as hydrogen bonds, hydrophobic contacts, and electrostatic forces. Binding energies were measured, and more negative values represented better affinities between ligand and protein.

MD simulations

The protocol for MD simulation started with parameterisation of the ligand by using the software package charmm-fit (CHArmm GUI Ligand Reader & Modeler), to generate CGenFF compatible topologies. These topologies were then converted to GROMACS format and combined with protein topologies that were generated with pdb2gmx using the force field (CHARMM36-jul2022) and the water model (TIP3P). Solvated protein-ligand complexes inside a dodecahedral box with TIP3P were used to saturate with water. The systems were neutralised and adjusted up to a 0.1 M NaCl concentration. After energy minimisation by the steepest descent algorithm with a force threshold of 1000 kJ/mol/nm, the system was allowed to come to equilibrium in two stages. The first stage was a 100 ps NVT ensemble at 300 K, with the V-rescale thermostat and particle - mesh Ewald (PME) electrostatics. The second stage was a 100 ps NPT ensemble at 1 bar (Parrinello-Rahman barostat). Production MD simulations were run for 100 ns with a time step of 1 fs. PME was still used for the long-range electrostatics and LINCS was used for hydrogen bond constraints, and all were

Table 1 — Docking grid parameters for molecular docking simulations (Vina configuration)

Receptor File	Exhaustiveness	Center X	Center Y	Center Z	Size X	Size Y	Size Z
5UBR.pdbqt	8	2.8056	6.9661	19.5203	78.0043	91.1126	92.8111
2Y3A.pdbqt	8	24.682398	-32.55131	-1.146029	73.3896	93.3902	99.4210
7LM2.pdbqt	8	19.3205	13.5310	19.4461	91.5131	103.6733	99.7970
8JN9.pdbqt	8	-28.7577	83.9669	121.6390	67.7579	61.8905	67.0195

maintained under constant temperature and pressure without restraints[22].

Post-simulation analysis (RMSD, RMSF, and Hydrogen bond analysis)

Root-mean-square deviation (RMSD) and calculated root-mean-square fluctuation (RMSF) calculations were used to determine the stability and flexibility of the protein-ligand complexes throughout the simulation. RMSD calculations, gmx rms module, were calculated for the protein backbone and heavy atoms of the ligand using the rms value at the end of minimization of the conformation changes, achieving a measure of the overall stability of the conformation. Per-residue RMSF analysis by gmx rmsf evaluated the atomic fluctuations, highlighting the rigid and flexible regions, particularly the ones close to the binding site, to understand the possible allosteric motions and dynamic stability. Hydrogen bond interactions between proteins and ligands were investigated using gmx hbond, and characteristics (donor-acceptor roles, occupancy, and geometric parameters of the hydrogen bonds, i.e., donor-acceptor distances and angles) were evaluated over time. This analysis showed the persistence and strength of important interactions that are critical for the complex stability of the system throughout the simulation[23].

Secondary structure evolution

The secondary structural elements were tracked along the simulation trajectory using gmx dssp which implements the Dictionary of Secondary Structure of Proteins (DSSP) algorithm. This analysis followed the motion of helix, sheet, turns and loops during the simulation to detect any significant structural transitions or unfolding events, giving insight into conformational structural transitions in secondary structure elements by ligand addition[24].

Binding free energy estimation (MM/GBSA)

The Molecular Mechanics Generalised Born Surface Area (MM/GBSA) method was used to estimate the binding free energy between protein and ligand using gmx_MMPBSA. The calculation used the igb = 5, Generalised Born implicit solvent model and sought to account for entropic contributions by including interaction entropy corrections. Snapshots were extracted from every 20 frames of the equilibrium trajectory, and energy components (van der Waals, electrostatics, polar and non-polarity solvation energy) were averaged to obtain the total binding free energy. This approach allowed a strong energetic characterisation of the binding interaction under near physiological conditions (T = 298.15 K) (T = 298.15 K)[25].

Principal component analysis (PCA) and free energy landscape (FEL)

To study large-scale collective motions, the Principal Component Analysis (PCA) was carried out with the gmx anaeig routine, based on the covariance matrix of atomic fluctuations in the fitted trajectory. The two most important eigenvectors were used to project the trajectory, therefore providing a two-dimensional representation (proj.xvg) of key motions. Subsequent mapping of the conformational space was performed using gmx sham, which was used to obtain a two-dimensional Free Energy Landscape (FEL) by estimating the Gibbs free energy based on the occupancy of the bins in the PC1-PC2 space. Custom Python scripts were also used to build high-resolution two and three-dimensional FEL plots. The two-dimensional FEL used hexagonal binning with Boltzmann-weighted energy estimation, while the three-dimensional FEL used Gaussian smoothing to increase the visual interpretability of energy basins and transition states. The landscapes were calculated at 300K, which allows visualisation of the dominant conformational states together with their relative stabilities[26].

Results

Targets of hydroxychloroquine and trimebutine

The prediction of targets of hydroxychloroquine and trimebutine was analysed in Swiss Target Prediction and grouped by functional class. For the hydroxychloroquine, most predicted targets (60.0 %) were from the Family A G-protein coupled receptor (GPCR) class. Other target classes were more evenly distributed among enzymes, electrochemical transporters, hydrolases, voltage-gated ion channels, and surface antigens (6.7-13.3%). For trimebutine, the predicted targets had more even distribution among several classes. The Family of GPCRs and proteases each represented 26.7% of the targets, followed by the kinases (20.0%), enzymes (13.3%) and small fractions of voltage-gated ion channels (6.7%) and writer proteins (6.7%) (Fig. 2).

Screening of therapeutic targets in alzheimer's disease

To study the possible therapeutic targets of hydroxychloroquine and trimebutine in Alzheimer's disease (AD), an analysis of gene intersection was carried out using the Venn diagram approach.

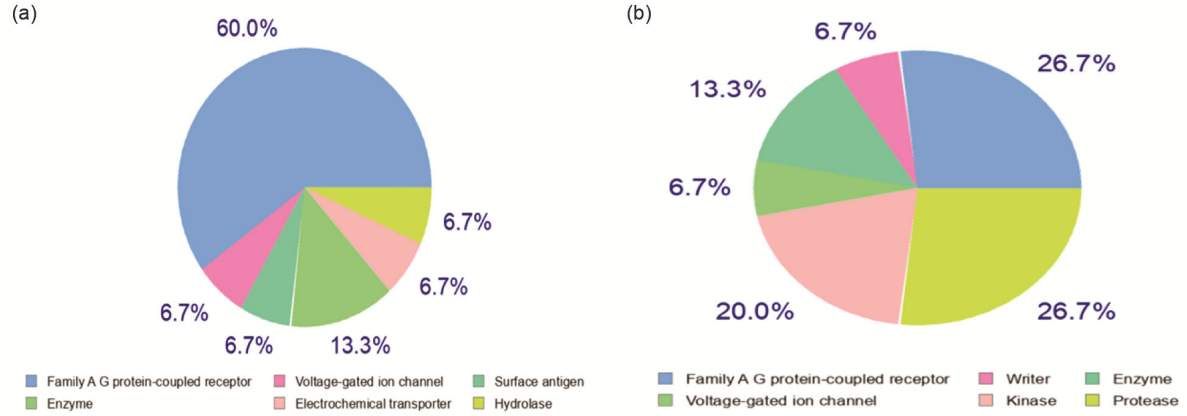

Fig. 2 — Predicted target class distribution of Hydroxychloroquine (a) and Trimebutine; and (b) using Swiss Target Prediction

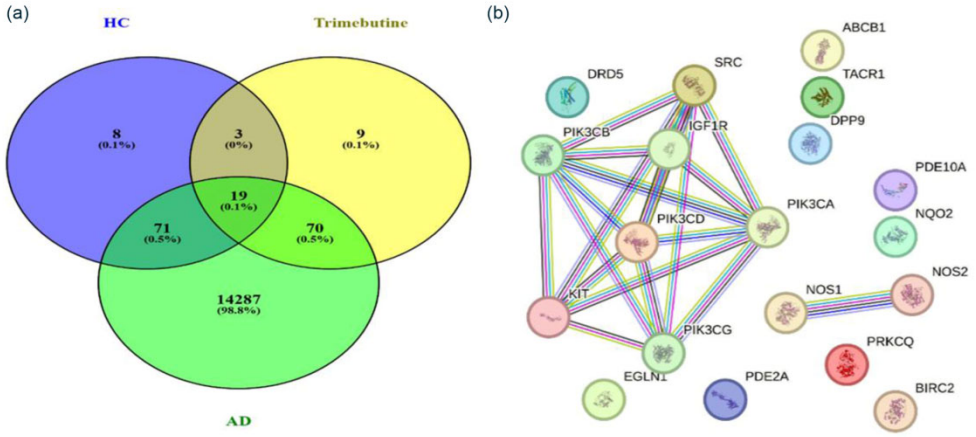

Fig. 3 — Venn diagram showing the overlap of predicted gene targets (a) Hydroxychloroquine, Trimebutine, and Alzheimer's; and (b) Protein-protein interaction (PPI) network of the 19 intersecting genes was constructed using the STRING databases

The common genes between disease and drug were 19 (0.1%) (Fig. 3a). The resulting protein-protein interaction network (PPI) had ten nodes and 32 edges and had an average node degree of 6.4. The average local clustering coefficient was 0.909, which shows that the gene network is dense and highly interactive. While the expected number of edges was 12, the number of observed 32 edges was a significant increase over this. A p-value calculated from a PPI enrichment test (PPI enrichment p-word only 5.52×10^{-7}) adds further support for the biological relevance and non-random nature of these interactions. The study synthesized together the predicted targets of hydroxychloroquine and trimebutine with Alzheimer's disease-associated genes and differentially expressed genes (DEGs) to discover core therapeutic targets that could mediate their neuroprotective actions.

Protein-protein interaction (PPI) network

A protein-protein interaction (PPI) network was employed from the STRING database to help explain functional relationships of shared targets of hydroxychloroquine and trimebutine in Alzheimer's disease (Fig. 3b). The network was characterized by a highly connected pattern with key hub nodes such as PIK3CA, PIK3CB, PIK3CD and SRC with the highest value of the interaction score (6), followed by PIK3CG and KIT (scores = 5) and IGF1R, NOS1 and NOS2 with lower connectivity (scores = 4 and 1, respectively). These genes have been implicated in important biological functions such as PI3K-Akt signalling, neuronal signalling, neuroinflammation and oxidative stress responses (Table 2) (Fig. 4).

Table 2 — Target gene selection for further molecular interaction analysis based on degree methods.

Rank	Name	Score
1	PIK3CD, PIK3CB, PIK3CA, SRC	6
5	PIK3CG, KIT	5
7	IGF1R	4
8	NOS1, NOS2	1

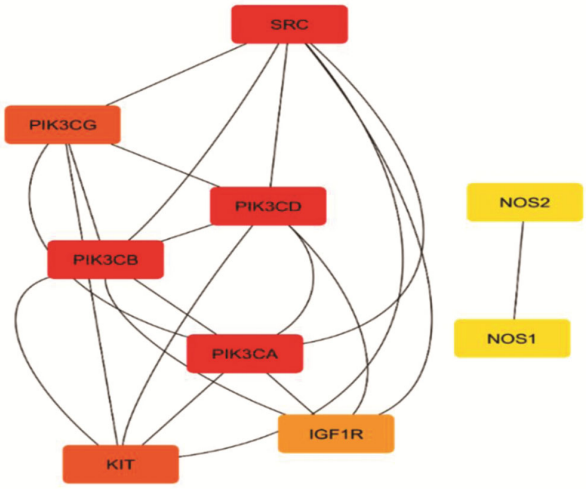

Fig. 4 — Hub gene ranking of overlapping target genes associated with Hydroxychloroquine, Trimebutine, and Alzheimer's disease

KEGG pathway enrichment associated with PI3K signalling, various biological processes

Enrichment analysis of the biological processes using the KEGG revealed the PI3K-Akt signaling pathway as one of the key pathways in the identified targets, such as PIK3CA, PIK3CB, PIK3CD, and SRC. This pathway was also connected with the VEGF-mediated angiogenesis (hsa04370) implying the possible connection between neuronal survival and vascular regulation. Further enrichment of longevity-regulating pathway (hsa04213) and EGFR tyrosine kinase inhibitor resistance pathway (hsa01521) shows that these targets are involved in more general cellular processes, including stress response, survival signaling, and adaptive processes.

These findings were reinforced by Gene Ontology (GO) analysis, as it identified biological processes involved with phosphatidylinositol-mediated signaling and positive regulation of protein kinase B (AKT) activity, crucial to cell survival, metabolism, and immune responses. PI3K isoform-dependent enrichment of cellular components of the PI3K complex and kinase-related cellular functions is another indicator of PI3K isoform involvement in cellular regulation of intracellular signaling by phosphoinositide phosphorylation. All in all, both KEGG and GO analyses indicate a similar signaling network involving PI3K/AKT activity, which could indicate that pathways pertaining to neuro-degeneration are co-regulated. Nonetheless, such findings are enrichment-based and can be understood as pointing to the potential involvement of the pathways as opposed to mechanistic evidence (Fig. 5).

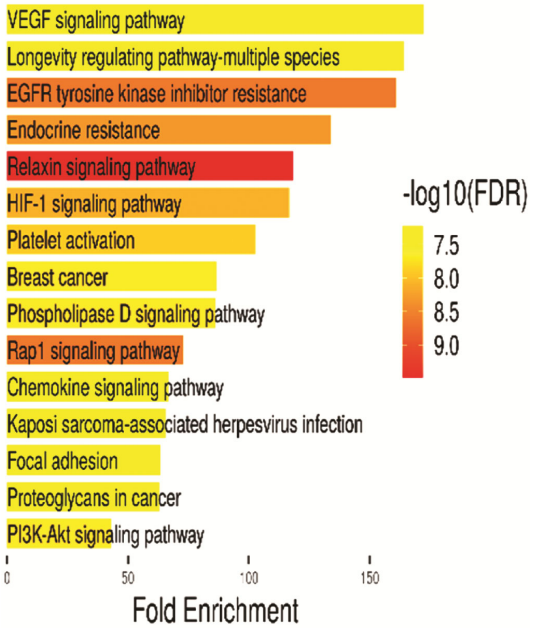

Fig. 5 — Bar plot of KEGG pathway enrichment analysis for common target genes of hydroxychloroquine and trimebutine in Alzheimer's

Gene expression analysis of molecular signature targets in alzheimer's disease brain regions associated with Aβ and Tau pathology

Gene expression analysis on important targets in the PI3K signaling pathway in Alzheimer's disease found that there were transcriptional alterations in the brain in several brain regions with modest, but non-significant, changes. Figures 6 and 7 are the results of the AlzData platform and offer the expression profiles of the entorhinal cortex, hippocampus, temporal and frontal cortex in AD and control subjects. PIK3CD had a minor increase in the temporal cortex (log2FC = 0.126), but this was not statistically significant (P = 0.22; FDR = 0.43), and there were even smaller changes in other areas. PIK3CB was mildly down regulated in the hippocampus (log2FC = -0.105) and frontal cortex (log2FC = - 0.059), but all results were not statistically significant (P> 0.2; FDR > 0.5). Similarly, PIK3CA exhibited weak trends of down-regulation, which were not statistically significant, and SRC observed weak up-regulation in chosen regions, which were not statistically significant.

Notably, as these genes were not significantly differentially expressed, their presence was maintained by their centrality in network topology and pathway enrichment and the fact that they are involved in important processes, including neuronal signaling, neuroinflammation and oxidative stress. It indicates that the pathway-level regulation, protein

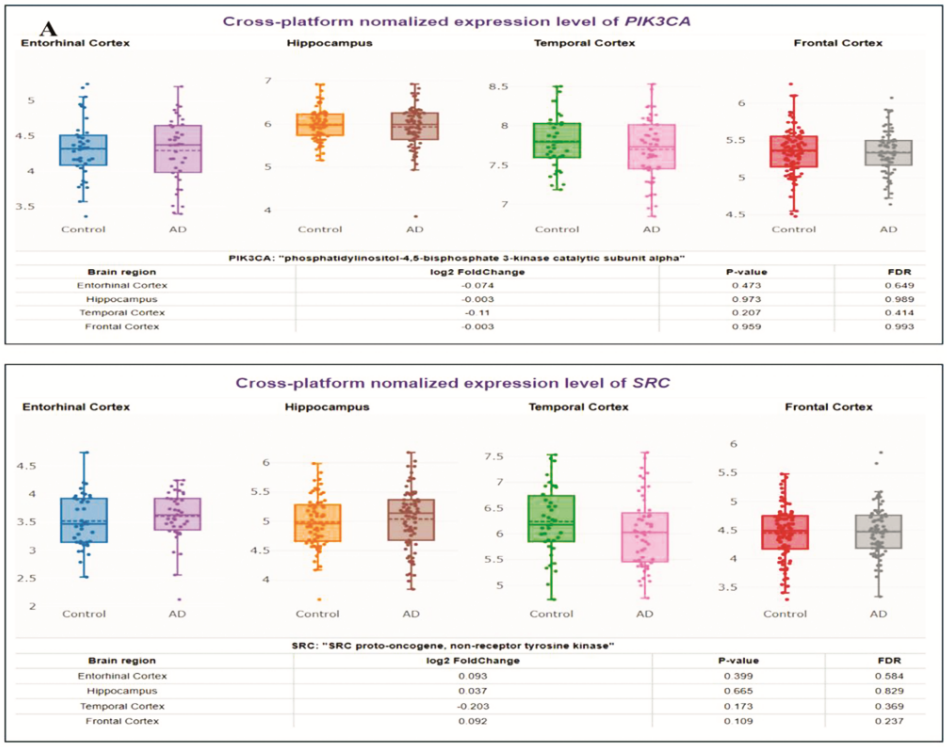

Fig. 6 — Cross-platform normalized expression levels of (a) PIK3CD; and (b) PIK3CB in the entorhinal cortex, hippocampus, temporal cortex, and frontal cortex

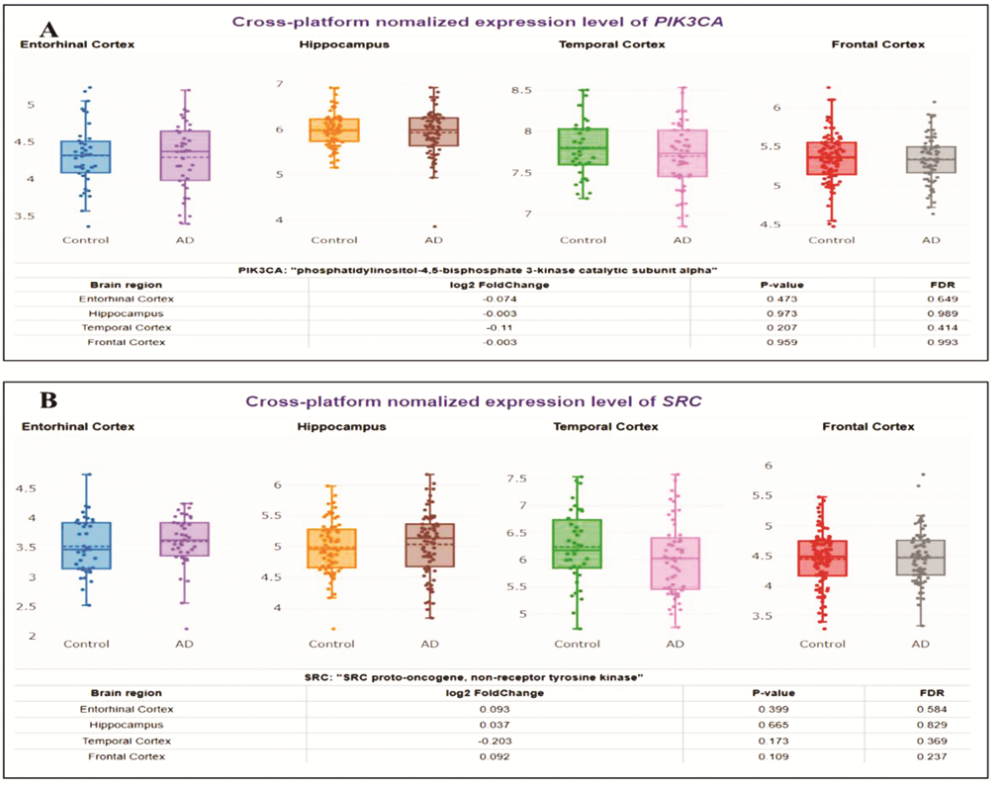

Fig. 7 — Cross-platform normalized expression levels of (a) PIK3CA; and (b) SRC in the entorhinal cortex, hippocampus, temporal cortex, and frontal cortex

Table 3 — Multi-dimensional evaluation of genes implicated in AD

Gene	eQTL	GWAS	PPI with AD Genes	Early DEG	Abeta Corr	Tau Corr	CFG
PIK3CD	2	0	PSEN1, PSEN2, MAPT	No	0.502	-0.106, ns	3
PIK3CB	2	0	APP, PSEN1, PSEN2, MAPT, APOE	NA	-0.073, ns	-0.429, ns	2
PIK3CA	2	0	APP, PSEN1, PSEN2, MAPT, APOE	NA	-0.170, ns	-0.485, ns	2
SRC	0	1	APP, PSEN1, PSEN2, MAPT, APOE	Yes	0.040, ns	-0.353, ns	3
PIK3CG	NA	0	APP, PSEN1, PSEN2, MAPT	Yes	0.814	0.673	3
KIT	0	0	PSEN1, PSEN2, MAPT, APOE	NA	NA	NA	1
IGF1R	2	0	PSEN1, PSEN2	NA	0.060, ns	-0.266, ns	2
NOS1	1	0	MAPT	NA	-0.043, ns	-0.171, ns	2
NOS2	3	0	-	NA	0.327	-0.455, ns	2

interactions, or post-translational mechanisms may contribute to their contribution to AD, instead of transcriptional changes. All in all, these results indicate that essential hub genes in the PI3K signaling pathway can have functional relevance in AD due to the interactions among genes at the systems level, which suggests the value of combining gene expression with network-based methods to gain a better insight into disease processes.

Functional genomics evidence supports PI3K family and related genes in AD pathology

Functional genomic investigations support the participation of the gene family of PI3K and related genetic factors in the neuropathogenesis of Alzheimer's disease (AD). The accompanying Table 3 provides a multidimensional appraisal of genes involved in AD, incorporating genetic, molecular and expression data. Several phosphoinositide 3-kinase genes are shown to have levels of evidentiary support in varying degrees, namely PIK3CD, PIK3CB, PIK3CA, and PIK3CG. PIK3CD sets important protein - protein interactions (PPIs) with most AD-associated proteins (PSEN1, PSEN2, MAPT) and its expression is robustly correlated with amyloid - beta ($r = 0.502$), resulting in a final CFG value of 3. SRC, even though it does not have quantified expression quantitative trait loci (eQTL) associations, registers one genome-wide association study (GWAS) hit, engages several AD proteins, and is identified as an early differentially expressed gene (DEG), and thus gains a CFG score of 3. PIK3CG deserves some attention due to these high correlations with both amyloid - beta ($r = 0.814$) and tau ($r = 0.673$) which are all coupled with significant PPI and early DEG status, also yielding a CFG score of 3. In contrast, genes like KIT and NOS1 have low supporting evidence with low CFG scores (1-2) and no significant expression correlation and interaction data. NOS2, without PPI information, has the maximum eQTL score (3) and displays a significant association with amyloid beta pathology ($r = 0.327$), thus confirming the involvement of this gene in AD-related inflammation. Additional genes (IGF1R, PIK3CB/PIK3CA in combination) show multiple PPIs and eQTL signals; however, they do not show significant correlation of expression or GWAS associations. Consequently, members of the PIK3 molecules and the SRC gene (PIK3CD) and the PIK3 gene (PIK3CG) emerge as interesting candidates for further studies for Alzheimer's investigation because they converge in very diverse lines of evidence whereas genes, for instance, like KIT seem to have lesser relevance.

Note: eQTL – Expression Quantitative Trait Loci, GWAS – Genome-Wide Association Study, PPI with AD Genes – Protein–Protein Interaction with Alzheimer's Disease Genes, Early DEG – Early Differentially Expressed Gene, Abeta Corr – Amyloid-beta Correlation, Tau Corr – Tau Correlation, CFG – Cumulative Functional Genomics Score

Protein validation

The analysis of the Ramachandran showed that all four protein structures exhibited satisfactory stereochemical quality. 5UBR, 7LM2, and 8JN9 exhibited a high percentage of residues in the most favored regions (approximately 88 - 92%) and no residues in disallowed regions, which represented excellent geometry in the backbone. 2Y3A showed a much lower percentage of favored residues (81.8%) and minimal occurrence of disallowed residues (0.3%), which is considered acceptable considering its considerable size. All structures show structural reliability and appropriateness for additional examination.

Molecular docking

The binding affinities of Trimebutine and Hydroxychloroquine to four target proteins (PDB IDs: 5UBR, 2Y3A, 7LM2, and 8JN9) were evaluated by

carrying out molecular docking simulations and the binding energies were calculated in kcal/mol (Table 4). In general, the two compounds exhibited moderate binding affinities, which were lower than their respective co-crystal ligands, reflecting the relatively weak interactions.

Trimebutine had the highest binding affinities with 5UBR and 2Y3A protein, with docking scores of -7.3 kcal/mol and -7.2 kcal/mol, respectively and a relatively lower affinity with the rest of the targets. Conversely, Hydroxychloroquine showed optimal binding with 2Y3A (-7.0 kcal/mol) and moderate binding with other targets (-6.4 to -6.5 kcal/mol). Nevertheless, compared to co-crystal and reference ligands, both compounds exhibited lower binding energies, which justifies that their interactions are weaker, in comparison to established inhibitors. However, binding energies greater than -6.0 kcal/mol indicate that there is a potential to interact reasonably with the target proteins (Figs. 8 & 9).

These data point to specific binding variability, and neither of the compounds has the binding strength that is comparable to established inhibitors. Thus, the interactions observed need to be viewed as moderate and supportive, but not definitive, and their potential therapeutic impact in Alzheimer's disease can be mediated by multi-target or pathway-based mechanisms, but not by strong single-target inhibition.

Out of the targets considered, 2Y3A was chosen to undergo further molecular dynamics (MD) simulations because of its consistently good and similar binding energies with both ligands, the existence of a defined binding pocket and the availability of a co-crystal ligand, which allows the validation of docking poses to be reliable. Moreover, the interaction profile of 2Y3A under dynamic conditions is stable during docking, which is why this protein is an ideal target to study the ligand and protein stability.

MD simulations

Root mean square deviation (RMSD)

The RMSD analysis (Fig. 10a-d) was used to evaluate the structural stability of the protein-ligand complexes over a 100 ns simulation period. The Hydroxychloroquine- 2Y3A complex had

Table 4 — Docking results of Hydroxychloroquine, Trimebutine, Co-crystal ligands and Reference

Targets	Binding Score			
	Hydroxychloroquine	Trimebutine	Co-crystal ligands	Reference
5UBR	-6.4	-7.3	-10.8	-9.0
2Y3A	-7.0	-7.2	-9.8	-7.7
7LM2	-6.5	-5.5	-8.2	-9.0
8JN9	-6.5	-6.0	-6.8	-8.9

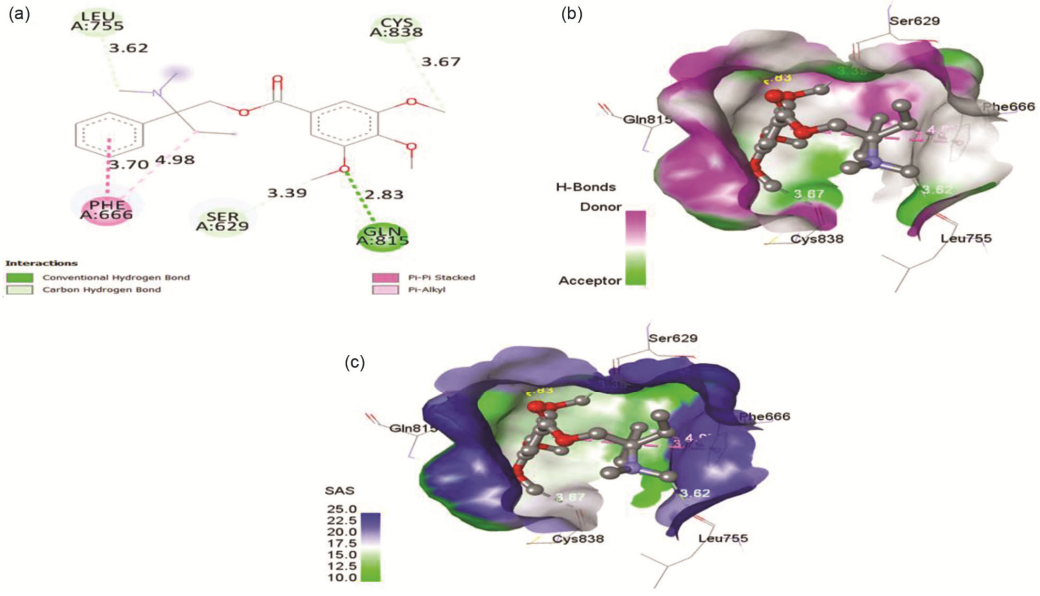

Fig. 8 — Hydroxychloroquine interaction with 2Y3A complex, where (a) represents 2D Interaction; (b) represents H-bonds; and (c) represents SAS Interaction

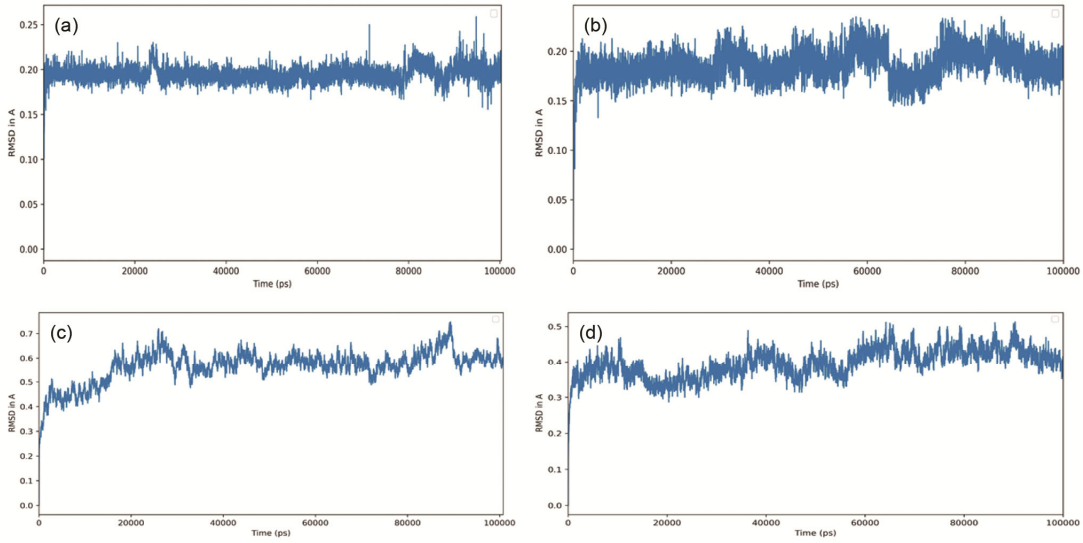

Fig. 9 — Trimebutine interaction with 5UBR complex, where (a) represents 2D Interaction; (b) represents H-bonds; (c) represents SAS Interaction

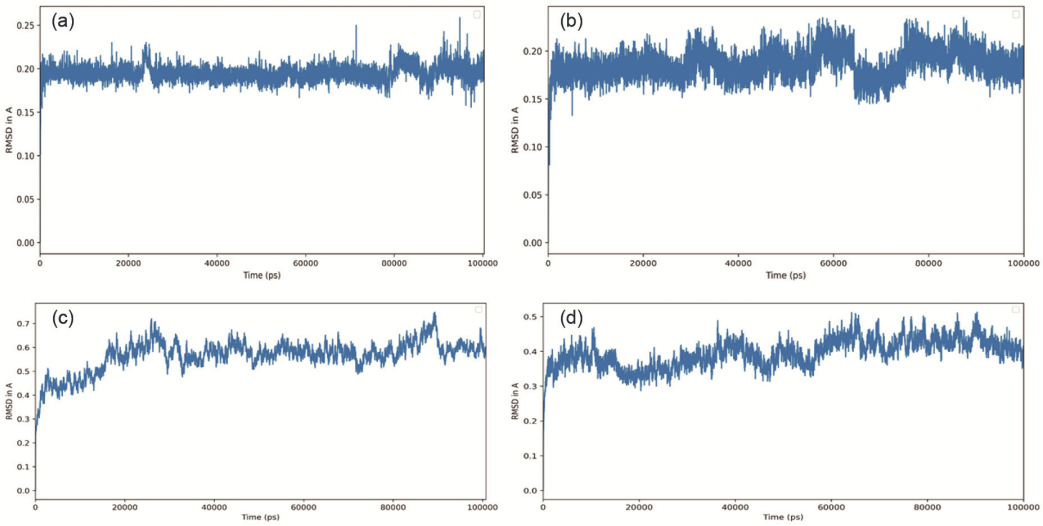

Fig. 10 — RMSD Profiles of Ligand and Protein Backbone, Ligand (a) & Protein Backbone (c) RMSD of Hydroxychloroquine-2Y3A Complex and Ligand (b) & Protein Backbone (d) RMSD of Trimebutine-5UBR Complex

comparatively low deviation (~0.18-0.22 nm) after equilibration, and this indicated that the structure of the complex had remained stable throughout the simulation period (Fig. 10a). Likewise, the apo-2Y3A system displayed similar changes (~0.15 0.21 nm) (Fig. 10b).

Conversely, the Trimebutine-5UBR complex exhibited more RMSD values (~0.35-0.70 nm), and this means that the conformational flexibility is high (Fig. 10c). The apo-5UBR system had intermediate deviations (~0.30 0.45 nm), which is in line with intrinsic protein dynamics without ligand binding (Fig. 10d). These observations are based on one simulation, though, and should be taken with caution.

Hydrogen bond analysis

To determine polar interactions that lead to the stability of a complex, hydrogen bond analysis was performed. The average number of hydrogen bonds that the Hydroxychloroquine-2Y3A complex had was 2-4 bonds, with some instances of 6, which showed relatively stable interactions throughout the simulation. Conversely, the Trimebutine-5UBR complex had fewer hydrogen bonds (1-3 on average) with irregular variations. These tendencies indicate that there are variations in the persistence of

interactions, but the conclusions about the stability are to be made in a qualitative manner because of the absence of replicate simulations (Fig. 11a & b).

Root mean square fluctuation (RMSF)

RMSF profiles (Fig. 11c & d) showed residue-level flexibility over both complexes. The hydroxyl-chloroquine-2Y3A system had a low average fluctuation (less than 0.35 nm), with the increased mobility limited to the N-terminal region and some selected loop regions (approximately residues 50-120 and 900-1000). The trimebutine-5UBR complex showed larger fluctuations, especially for loops that are exposed on the surface, with peaks greater than 0.45 nm. This increased flexibility is in line with the higher RMSD values recorded and may reflect that trimebutine binding causes local conformational rearrangements instead of rigid stabilisation.

Secondary structure evolution

The analysis of the secondary structure (Fig. 12a & b) revealed that the overall structural integrity of both complexes was mostly maintained during the simulation. The Hydroxychloroquine 2Y3A complex

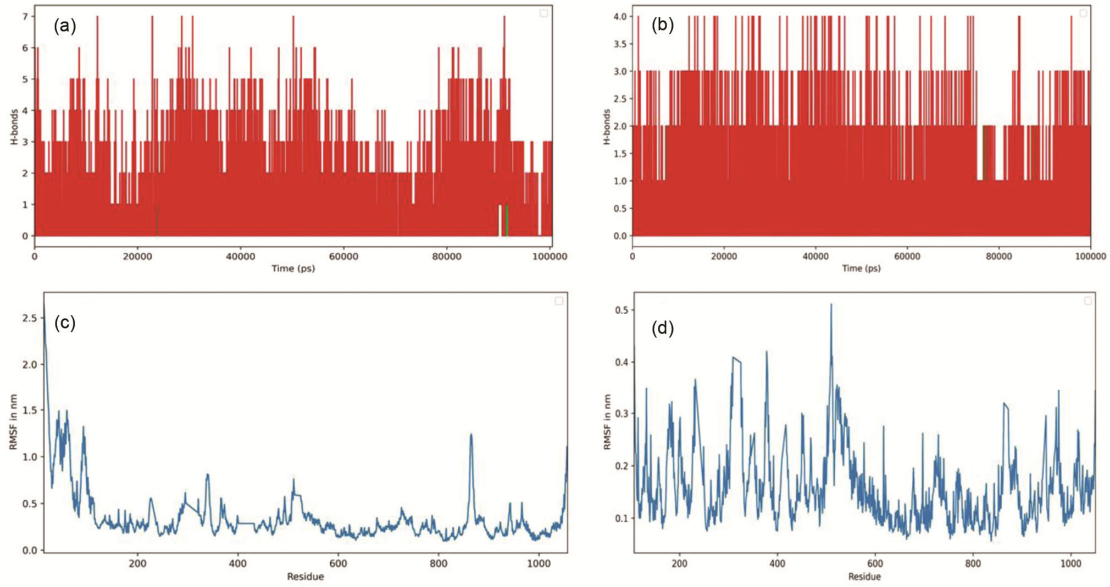

Figure 11 — Hydrogen bonding interactions and root mean square fluctuation (RMSF) profiles, (a) Time-resolved hydrogen bonds in hydroxychloroquine-2Y3A complex, (b) Time-resolved hydrogen bonds in trimebutine-5UBR complex, (c) Per-residue RMSF of hydroxychloroquine-2Y3A complex, (d) Per-residue RMSF of trimebutine-5UBR complex

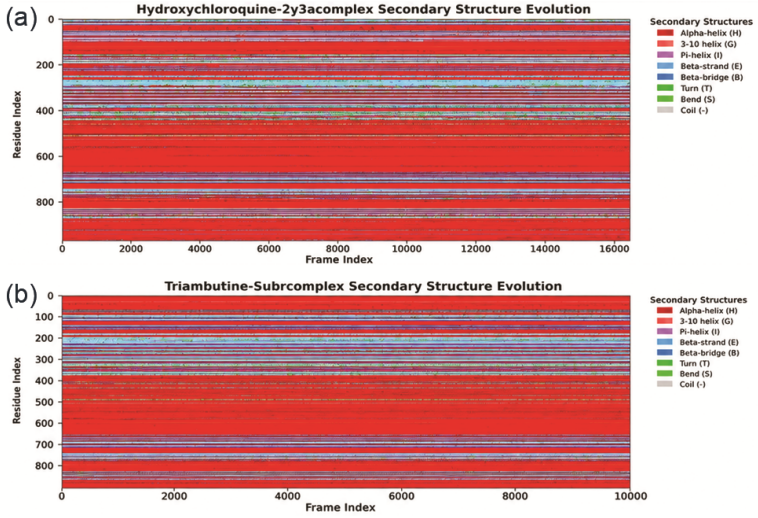

Fig. 12 — Secondary structure evolution during molecular dynamics simulations, (a) Secondary structure dynamics of hydroxychloroquine-2Y3A complex, and (b) Secondary structure dynamics of trimebutine-5UBR complex

exhibited a small increment in the retention of the 2Y3A complex of the alpha helix peptide content, but the Trimebutine 5UBR complex had a slight increment of the coil regions, in line with its increased flexibility. These variations give encouraging, yet not definitive, hints into structural behaviour.

Free energy landscape (FEL)

Free energy landscape (Fig. 13a-d) indicated that the Hydroxychloroquine-2Y3A complex was in a relatively well-defined low-energy basin, and the Trimebutine-5UBR complex was in a variety of shallow minima. This can be taken as a sign of conformational preference variation, but such interpretations must be handled with care since there are no replicate simulations.

Principal component analysis (PCA)

PCA plots (Fig. 14a & b) captured the essential complex motion for the complexes. The hydroxychloroquine-2Y3A system had a more confined conformational space, because it clustered

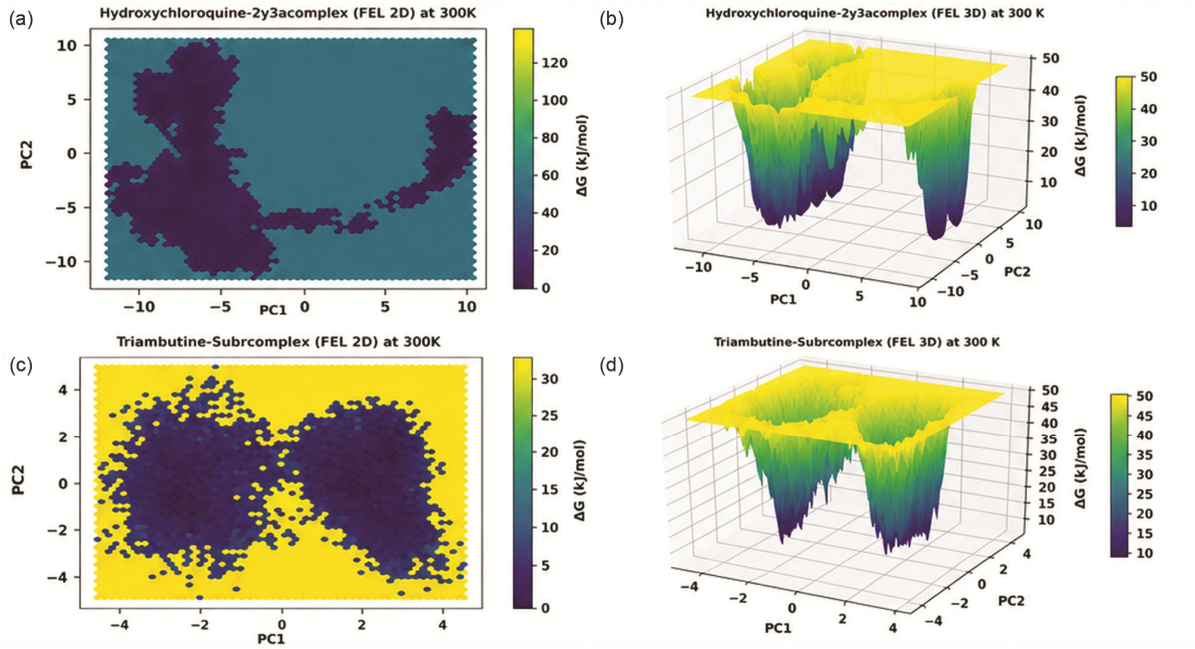

Figure 13 — Free energy landscape (FEL) analysis of molecular dynamics trajectories, (a) FEL plot of hydroxychloroquine-2Y3A complex, (b) FEL plot of hydroxychloroquine-2Y3A complex, (c) FEL plot of trimebutine-5UBR complex, (d) FEL plot of trimebutine-5UBR complex

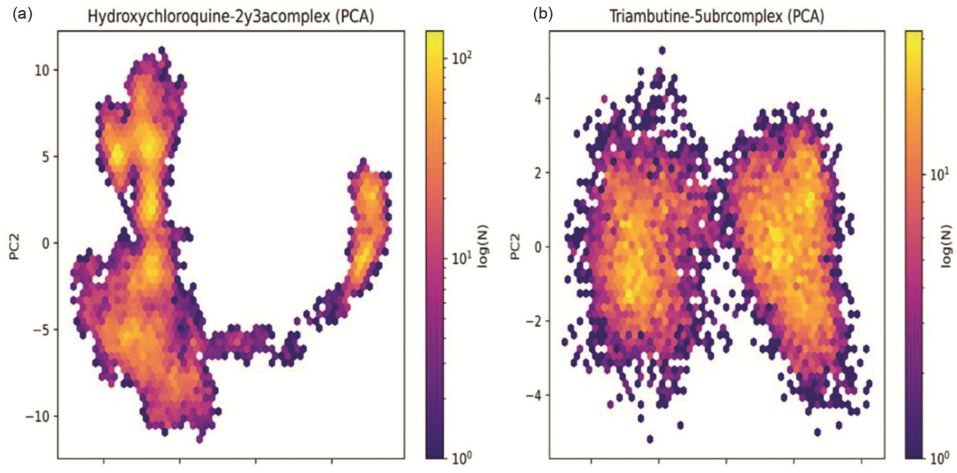

Figure 14 — Principal component analysis (a) (PCA) Plot of hydroxychloroquine-2Y3A complex; and (b) PCA Plot of trimebutine-5UBR complex

into lesser numbers of well-defined minima, suggesting the presence of stable global dynamics. In contrast, the trimebutine-5UBR complex was able to explore more conformational space, indicating more conformational flexibility and less conformational constraint.

Simulation outcomes in MD are usually in line with docking, where the two compounds had moderate binding affinities with the targets. Interestingly, Hydroxychloroquine-2Y3A complex exhibited relatively stable behaviour during simulation despite the moderate docking scores, and Trimebutine-5UBR exhibited higher flexibility. These results reveal that docking gives a preliminary indication of binding potential, whereas MD simulations can provide further information on dynamic behaviour. Nevertheless, such results can only be discussed as initial and preliminary since only single simulations were conducted.

Screening of hydroxychloroquine and trimebutine characteristics

Computational models were used to determine the membrane permeability of Hydroxychloroquine and Trimebutine. The binding free energy of hydroxychloroquine to DOPC membranes (-4.19 kcal/mol) was more favourable than that of Trimebutine (-2.77 kcal/mol) was more favorable, indicating a relatively greater affinity to the membrane. In the same manner, the logarithmic permeability coefficients in various models (BLM, BBB, Caco-2, and PAMPA-DS) were a bit more positive with Hydroxychloroquine (Table 5, and Fig. 15). These findings suggest that there could be permeability variations; they are, however, predicted models and need additional confirmation (Table 5).

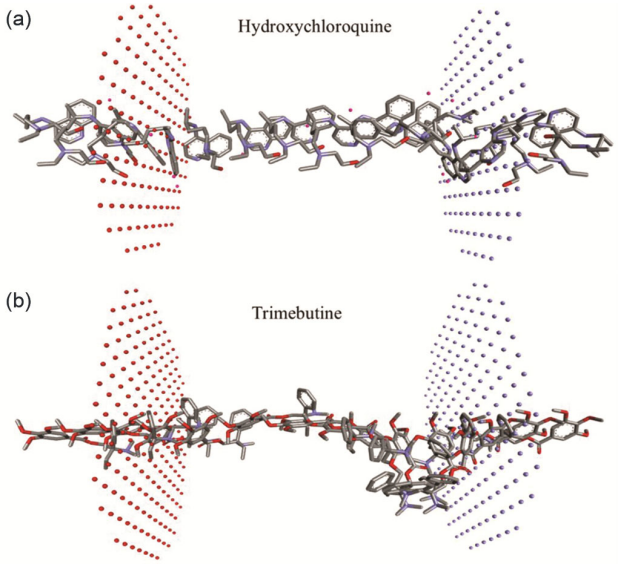

Fig. 15 — Cell permeability representation of the translocation pathway of hydroxychloroquine and trimebutine

Table 5 — Cell permeability analysis of hydroxychloroquine and trimebutine

Cell permeability	Hydroxychloroquine	Trimebutine
Free energy of binding (DOPC)	-4.19 kcal/mol	-2.77 kcal/mol
Log of perm. coeff. - BLM	-1.20	-1.25
Log of perm. coeff - BBB (Po)	-3.32	-3.33
Log of perm. coeff - CACO2 (Po)	-3.79	-3.80
Log of perm. coeff - PAMPA-DS (Po)	-2.34	-2.38

Discussion

This study uses PI3K as one of the targets (PIK3CA, PIK3CB, PIK3CD) and SRC as the main target due to network pharmacology, demonstrating the significance of the PI3K-Akt signaling pathway in Alzheimer's disease. These receptors have been found to control neuronal survival, synaptic plasticity, autophagy, and neuroinflammatory events, which are key processes in AD pathogenesis. Though the observed changes in gene expression were not statistically significant, high network connectivity and pathway enrichment indicate that these proteins could be functional regulators on the signalling scale, but not via transcriptional changes. The *in silico* findings are supported by existing experimental evidence. Hydroxychloroquine has been demonstrated to regulate intracellular signaling and inflammatory responses, such as JAK/STAT and other cell survival responses, reduce neuroinflammation, increase amyloid-β clearance, and increase synaptic plasticity in AD models(13). The mechanistically consistent effect of these is consistent with modulation of PI3K- and SRC-associated signaling cascades, which have upstream roles in the regulation of neuronal and immune responses.

On the same note, Trimebutine has shown a high level of acetylcholinesterase inhibition *in vitro*, which means that it can modulate cholinergic signaling, which is one of the main pathological characteristics of AD(12). The present network analysis further indicates that trimebutine can also bind PI3K-related targets, which indicates that there is a possibility of the dual mechanism between the neurotransmission and survival signalling pathways. In general, this combination of network pharmacology prediction

and experimental and clinical data confirms the hypothesis that the possible neuroprotective effects of these drugs can be explained by the modulated PI3K and SRC signaling. Nevertheless, these mechanistic insights are predictive and additional experiments are necessary to establish their contribution in the Alzheimer disease.

Conclusion

Pathway enrichment and network analyses identified Trimebutine and Hydroxychloroquine as potential targets in Alzheimer's disease pathophysiology, including cholinergic pathways, autophagy processes, and the PI3K-Akt signalling pathway. These relationships are based on computational predictions and should be considered hypotheses rather than proof. In molecular dynamics simulations, hydroxychloroquine revealed stable interaction patterns and favourable projected central nervous system permeability and lysosomal localization, indicating neuroprotective benefits. Trimebutine had moderate target engagement, PI3K-related protein connections, and expected acetylcholinesterase activity, but poorer dynamic stability. These data show that these chemicals may affect numerous Alzheimer's disease pathways, although the mechanisms are still speculative and need additional testing.

Limitations of the study and Future prospects

This *in silico* investigation is limited by the lack of *in vivo* validation, which is required to determine efficacy, safety and blood-brain barrier permeability. Molecular dynamics simulations were conducted as individual runs without repeats or statistical validation. Consequently, the findings regarded as provisional and require more validation. Future research should include experimental assessments, animal models and potential combinatory strategies to assess the multi-target therapeutic potential of trimebutine and hydroxychloroquine for Alzheimer's disease.

Acknowledgement

We thank the Department of Pharmacology, KLE College of Pharmacy, Bengaluru-560010, for providing resources and computational support to conduct this research.

Conflict of interest

All authors declare no conflict of interests.

References

1 Mucke L, Neuroscience: Alzheimer’s disease. *Nature*, 461 (2009) 895.

2 World Health Organization, Dementia. *WHO Fact Sheet*, (2026) [accessed 15 April 2026].

3 Lastuka A, Bliss E, Breshock MR, Iannucci VC, Sogge W, Taylor KV, Pedroza P & Dieleman JL, Societal costs of dementia: 204 countries, 2000–2019. *J Alzheimers Dis*, 101 (2024) 277.

4 World Health Organization, Dementia: Number of people affected to triple in next 30 years. *WHO News*, (2017) [accessed 5 July 2025].

5 Singh N, Kumar K, Kaur S, Kandpal A, Yadav HN, Singh D, Chopra DS, Jaggi AS, Kumar A & Mani V, Pathophysiology and diagnosis of Alzheimer’s disease: Past and recent developments. *Apple Academic Press*, (2025).

6 Verma M, Shukla S, Shrivastava S & Puranik N, Neurodegenerative disorder: An overview. In: *Proteostasis: Investigating Molecular Dynamics in Neurodegenerative Disorders*, Springer, (2025) 1.

7 Rahman A, Jaiswal A, Keshari P & Singh DK, Alzheimer’s: Epidemiology, pathophysiology, diagnosis, and treatments. In: *Proteostasis: Investigating Molecular Dynamics in Neurodegenerative Disorders*, Springer, (2025) 39.

8 Al-Bari MAA, Chloroquine analogues in drug discovery: New directions of uses, mechanisms of actions and toxic manifestations from malaria to multifarious diseases. *J Antimicrob Chemother*, 70 (2015) 1608.

9 Delvaux M & Wingate D, Trimebutine: Mechanism of action, effects on gastrointestinal function and clinical results. *J Int Med Res*, 25 (1997) 225.

10 Ballard C, Aarsland D, Cummings J, O’Brien J, Mills R, Molinuevo JL, Fladby T, Williams G, Doherty P & Corbett A, Drug repositioning and repurposing for Alzheimer disease. *Nat Rev Neurol*, 16 (2020) 661.

11 Plantone D & Koudriavtseva T, Current and future use of chloroquine and hydroxychloroquine in infectious, immune, neoplastic, and neurological diseases: A mini-review. *Clin Drug Investig*, 38 (2018) 653.

12 Akkaya D, Seyhan G, Sari S & Barut B, *In vitro* and *in silico* investigation of FDA-approved drugs to be repurposed against Alzheimer’s disease. *Drug Dev Res*, 85 (2024) 1.

13 Varma VR, Desai RJ, Navakkode S, Wong LW, Anerillas C, Loeffler T, Schilcher I, Mahesri M, Chin K, Horton DB, Kim SC, Gerhard T, Segal JB, Schneeweiss S, Gorospe M, Sajikumar S & Thambisetty M, Hydroxychloroquine lowers Alzheimer’s disease and related dementias risk and rescues molecular phenotypes related to Alzheimer’s disease. *Mol Psychiatry*, 28 (2023) 1312.

14 Boziki M, Grigoriadis N, Papaefthymiou A, Doulberis M, Polyzos SA, Gavalas E, Deretzi G, Karafoulidou E, Kesidou E, Taloumtzis C, Theotokis P, Sofou E, Katsinelos P, Vardaka E, Fludaras I, Touloumtzi M, Koukoufiki A, Simeonidou C, Liatsos C & Kountouras J, The trimebutine effect on Helicobacter pylori-related gastrointestinal tract and brain disorders: A hypothesis. *Neurochem Int*, 144 (2021) 104938.

15 Gfeller D, Grosdidier A, Wirth M, Daina A, Michielin O & Zoete V, SwissTargetPrediction: A web server for target prediction of bioactive small molecules. *Nucleic Acids Res*, 42 (2014) W32.

16 Safran M, Dalah I, Alexander J, Rosen N, Iny Stein T, Shmoish M, Nativ N, Bahir I, Doniger T, Krug H, Sirota-Madi A, Olender T, Golan Y, Stelzer G, Harel A & Lancet D, GeneCards Version 3: The human gene integrator. *Database*, 2010 (2010) 1.

17 Franceschini A, Szklarczyk D, Frankild S, Kuhn M, Simonovic M, Roth ACJ, Lin J, Minguez P, Bork P, von Mering C & Jensen LJ, STRING v9.1: Protein-protein interaction networks, with increased coverage and integration. *Nucleic Acids Res*, 41 (2013) D808.

18 Mousavian Z, Khodabandeh M, Sharifi-Zarchi A, Nadafian A & Mahmoudi A, StrongestPath: A Cytoscape application for protein–protein interaction analysis. *BMC Bioinformatics*, 22 (2021) 352.

19 Marco-Ramell A, Palau-Rodriguez M, Alay A, Tulipani S, Urpi-Sarda M, Sanchez-Pla A & Andres-Lacueva C, Evaluation and comparison of bioinformatic tools for the enrichment analysis of metabolomics data. *BMC Bioinformatics*, 19 (2018) 1.

20 Yan B, Liao P, Zhang W, Han Z, Wang C, Chen F & Lei P, Identification of key fatty acid metabolism-related genes in Alzheimer's disease. *Mol Neurobiol*, 62 (2025) 9399.

21 Gote S, Thapa S, Dubey S, Nargund S & Biradar MS, Computational investigation of quinazoline derivatives as Keap1 inhibitors for Alzheimer's disease. *Inform Med Unlocked*, 41 (2023) 101334.

22 Van Der Spoel D, Lindahl E, Hess B, Groenhof G, Mark AE & Berendsen HJC, GROMACS: Fast, flexible, and free. *J Comput Chem*, 26 (2005) 1701.

23 Shukla R & Tripathi T, Molecular dynamics simulation of protein and protein–ligand complexes. In: *Computer-Aided Drug Design*, Springer, (2020) 133.

24 Gorelov S, Titov A, Tolicheva O, Konevega A & Shvetsov A, DSSP in GROMACS: Tool for defining secondary structures of proteins in trajectories. *J Chem Inf Model*, 64 (2024) 3593.

25 Dong L, Qu X, Zhao Y & Wang B, Prediction of binding free energy of protein–ligand complexes with a hybrid molecular mechanics/generalized born surface area and machine learning method. *ACS Omega*, 6 (2021) 32938.

26 Papaleo E, Mereghetti P, Fantucci P, Grandori R & De Gioia L, Free-energy landscape, principal component analysis, and structural clustering to identify representative conformations from molecular dynamics simulations: The myoglobin case. *J Mol Graph Model*, 27 (2009) 889.